Secure Transmission Design with Strong Channel Correlation for Passive/Active RIS Communications

Jun Sun, Junjie Li, Wanming Hao, Xiaomin Mu, Zheng Chu, and Pei Xiao

***Abstract*—Physical layer security (PLS) is a promising technique to improve the security of wireless communications. However, when the legitimate user's and eavesdropper's channels are strongly correlated, directly applying PLS might no longer be a valid approach. In this paper, by introducing the reconfigurable intelligent surface (RIS), we study how to design access point (AP) and RIS beamforming and deploy RIS to improve the security under strong channel correlation. Furthermore, by taking into consideration the "multiplicative fading" effect, we formulate the secrecy rate (SR) maximization problem in the passive and active RIS cases. Next, we propose a semidefinite program (SDR)-based alternative optimization (AO) algorithm for each case, respectively. However, the computational complexity of the SDR approach is prohibitive for the large-size RIS. To tackle this issue, we respectively develop the low-complexity minorization maximization-based and primal-dual subgradient-based AO algorithms for two cases. Finally, we analyze the effect of the RIS deployment on the SR, and simulations results demonstrate the effectiveness of the proposed schemes.**

***Index Terms*—Reconfigurable intelligent surface, physical layer security, channel correlation.**

I. Introduction

With the rapid development of the fifth-generation (5G) mobile communications, academia and industry are looking for more cutting-edge technologies to meet the needs of B5G and 6G applications, including ultra-high speed rate, energy efficiency, security and ultra-low delay [1]. Because of the broadcast characteristics of wireless communication, it is vulnerable to information leakage and attack [2]. Compared with traditional encryption security scheme, physical layer security (PLS) has attracted increasing attention due to its ability to safeguard wireless transmissions without incurring additional computational complexity and communication overhead [3]. Applying PLS, the quality of signals received by illegal users can be effectively reduced by optimizing access point (AP) beamforming (BF). However, when the legitimate user's channel has strong correlation with the eavesdropper's (Eve's) as shown in Fig. 1(a), the achievable secrecy rate (SR) is very limited by conventional PLS techniques.

Recently, reconfigurable intelligent surface (RIS) has attracted great attention as a promising technology for future wireless communications. Specifically, RIS consists of a large number of low-cost passive reflecting elements, and each element can independently adjust the amplitude and phase of the incoming signals [4], which effectively overcomes the blockage effect and improves the system capacity. However, due to the effect of the "multiplicative fading" of the cascaded RIS channel, the improved performance is limited, especially when there exists direct link between users and AP. To circumvent this problem, [5] propose a new active RIS structure, and each reflecting element or multiple elements is equipped with a power amplifier, which effectively improve the SR. In comparison, the hardware overhead of active relay is higher than that of active RIS. For example, the relay needs digital-to-analog and analog-to-digital converters, mixers, power amplifiers and so on [6], and full duplex relay also need to consider the self-interference problem, which requires the large overhead. Whereas, the active RIS only needs the simple power amplification and diodes, and the overhead is small. Meanwhile, Active RIS outperforms relay in terms of performance and overhead under the same condition [7]. In addition, RIS can also improve the overall security of the system by providing additional communication links by bypassing Eves [8]. There have been several works considering the RIS-aided secure communications [9] [10], but they do not study the effect of the RIS deployment and active RIS on the SR, especially when the legitimate user and Eve have strongly correlated channels.

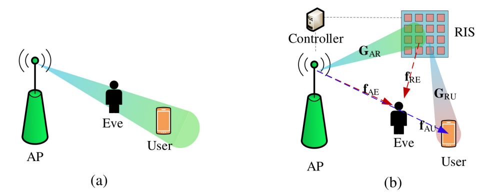

Fig. 1. Basic secure communication model under strong channel correlation: (a) without RIS, (b) with RIS.

Against this background, in this paper, we study the joint AP and passive/active RIS BF design problem under the strong channel correlation among legitimate user and Eve. Firstly, we formulate the SR maximization problem both the passive and active RIS cases, respectively. For the passive RIS case, we first propose an alternative optimization (AO) algorithm based on the semidefinite relaxation program (SDR) technique. To avoid the high computational complexity and rank-one constraint caused by SDR, we propose a low-complexity minorization maximization (MM)-based AO algorithm. For the active RIS case, we also propose a similar SDR-based AO algorithm, and then develop a primal-dual subgradient (PDS)-based AO algorithm that avoids applying the SDR approach to solve RIS BF, which can effective reduce the complexity for a large-size RIS. Meanwhile, we analyze the effect of the RIS deployment on the SR in simulations.

J. Sun, J. Li, W. Hao and X. Mu are with the School of Electrical and Information Engineering, Zhengzhou University, Zhengzhou 450001, China (e-mail: sunjun@zut.edu.cn, 202012592017620@gs.zzu.edu.cn, {iewmhao,iexmmu}@zzu.edu.cn).

Z. Chu and P. Xiao are 5GIC & 6GIC, Institute for Communication Systems (ICS), University of Surrey, Guildford GU2 7XH, UK. (Email: Andrew.chuzheng7@gmail.com, p.xiao@surrey.ac.uk)

II. System Model and Problem Formulation

As shown in Fig. 1(b), we consider a downlink RIS secure communication scenario. We assume that the AP is consisted of an M_t-antenna uniform linear array to serve a single-antenna legitimate user in presence of a single-antenna Eve, and the RIS is an N_t-element uniform planar array. The channel links from AP to RIS, from AP to legitimate user, from AP to Eve, from RIS to legitimate user, and from RIS to Eve are denoted as $\mathbf{G}_{AR} \in \mathbb{C}^{N_t\times M_t}$, $\mathbf{h}_{AU} \in \mathbb{C}^{M_t\times 1}$, $\mathbf{h}_{AE} \in \mathbb{C}^{M_t\times 1}$, $\mathbf{f}_{RU} \in \mathbb{C}^{N_t\times 1}$, and $\mathbf{f}_{RE} \in \mathbb{C}^{N_t\times 1}$, respectively. The classic S-V mmWave channel model is applied [11], i.e., $\mathbf{h}_{Aj} = \sqrt{M_t/L_{Aj}}\sum_{l=1}^{L_{Aj}} \alpha_{Aj}^{(l)}\mathbf{a}(\varphi_{Aj}^{(l)})$, $j \in \{U, E\}$, where L_{Aj} denotes the number of paths from AP to receiver j, $\mathbf{a}(\varphi_{Aj}^{(l)}) = \frac{1}{\sqrt{M_t}}e^{-jkd\sin(\varphi_{Aj}^{(l)})[0,\ldots,M_t-1]^T}$, $\varphi_{Aj}^{(l)}$ represents the azimuth angle for the transmitter of the l-th path, $\alpha_{Aj}^{(l)}$ represents the channel gain of the l-th path, $k = 2\pi/\lambda$, d and λ represent antenna spacing and wavelength. Other channels have the similar expressions. Since the power of the line-of-sight (LoS) path of the mmWave channel is the main component [11], $\mathbf{h}_{AU}$ and $\mathbf{h}_{AE}$ are strong correlation when the legitimate user and the Eve have the same azimuth angle of the AP (i.e., $\varphi_{AU} = \varphi_{AE}$) , and their correlation can be approximated as $\sqrt{(a_{Aj}^{LoS})^2/(\sum_{l=1}^{L_{Aj}}(a_{Aj}^{(l)})^2)}$, where a_{Aj}^{LoS} denotes the gain of the LoS path.

For the passive RIS, the signals received by the user and Eve can be expressed

$$y_j = \left(\mathbf{h}_{Aj}^H + \mathbf{f}_{Aj}^H\boldsymbol{\Theta}\mathbf{G}_{AR}\right)\mathbf{x} + n_j, j \in \{U, E\}, \tag{1}$$

where $\mathbf{x} = \mathbf{w}s$ is the precoding symbol transmitted by the AP, $\mathbf{w} \in \mathbb{C}^{M_t\times 1}$ denotes the precoding vector, s is the confidential information satisfying $\mathbb{E}\left\{|s|^2\right\} = 1$, $n_U \sim \mathcal{CN}\left(0, \sigma_U^2\right)$ and $n_E \sim \mathcal{CN}\left(0, \sigma_E^2\right)$ are the white Gaussian noise with zero mean and variance σ_U^2 and σ_E^2 at the user and Eve, respectively. $\boldsymbol{\Theta} = \mathrm{diag}\left(\boldsymbol{\theta}\right)$ symbolizes the reflection coefficient matrix of the RIS. Here, we define $\boldsymbol{\theta} = [\theta_1, \ldots, \theta_{N_t}]^T$ and $\theta_n = \eta_n e^{j\vartheta_n}$, where η_n and ϑ_n represent the amplitude and phase shift of the n-th element, respectively. To maximize the reflection efficiency, we set the reflection amplitude $\eta_n = 1$.

For the active RIS, the signals received by user and Eve are represented as [12]

$$\hat{y}_j = \left(\mathbf{h}_{Aj}^H + \mathbf{f}_{Aj}^H\boldsymbol{\Theta}\mathbf{G}_{AR}\right)\mathbf{x} + \mathbf{f}_{Aj}^H\boldsymbol{\Theta}\mathbf{n}_R + n_j, j \in \{U, E\}, \tag{2}$$

where $\mathbf{n}_R \sim \mathcal{CN}\left(\mathbf{0}, \sigma_R^2\mathbf{I}\right)$ represents the thermal noise generated by RIS. Each element of active RIS is equipped with an amplifier, and thus the reflection amplitude $\eta_n \geq 1$.

For the passive RIS, the SR maximization problem can be formulated as follows.

$$\begin{aligned}\mathcal{P}_0 : \max_{\mathbf{w},\boldsymbol{\Theta}} &\left[\log_2\left(1+\left|\left(\mathbf{h}_{AU}^H+\mathbf{f}_{AU}^H\boldsymbol{\Theta}\mathbf{G}_{AR}\right)\mathbf{w}\right|^2/\sigma_U^2\right)\right.\\ &\left.- \log_2\left(1+\left|\left(\mathbf{h}_{AE}^H+\mathbf{f}_{AE}^H\boldsymbol{\Theta}\mathbf{G}_{AR}\right)\mathbf{w}\right|^2/\sigma_E^2\right)\right]^+ \quad (3a)\\ \text{s.t. } &\|\mathbf{w}\|^2 \leq P_{\max},\ |\boldsymbol{\theta}_n| = 1, \forall n, \quad (3b)\end{aligned}$$

where $P_{\max}$ symbolizes the maximum transmit power of AP.

For the active RIS, the SR maximization problem can be formulated as follows.

$$\begin{aligned}\mathcal{P}_1 : \max_{\mathbf{w},\boldsymbol{\Theta}} &\left[\log_2\left(1 + \frac{\left|\left(\mathbf{h}_{AU}^H + \mathbf{f}_{AU}^H\boldsymbol{\Theta}\mathbf{G}_{AR}\right)\mathbf{w}\right|^2}{\left\|\mathbf{f}_{AU}^H\boldsymbol{\Theta}\mathbf{n}_R\right\|^2 + \sigma_U^2}\right)\right.\\ &\left.- \log_2\left(1 + \frac{\left|\left(\mathbf{h}_{AE}^H + \mathbf{f}_{AE}^H\boldsymbol{\Theta}\mathbf{G}_{AR}\right)\mathbf{w}\right|^2}{\left\|\mathbf{f}_{AE}^H\boldsymbol{\Theta}\mathbf{n}_R\right\|^2 + \sigma_E^2}\right)\right]^+ \quad (4a)\\ \text{s.t. } &\|\mathbf{w}\|^2 + \|\boldsymbol{\Theta}\mathbf{G}_{AR}\mathbf{w}\|^2 + \sigma_R^2\|\boldsymbol{\Theta}\|^2 \leq \hat{P}_{\max}, \quad (4b)\\ &|\theta_n| \leq \eta_n, \forall n, \quad (4c)\end{aligned}$$

where $\hat{P}_{\max}$ symbolizes the maximum sum transmit power constraint at AP and RIS,[1] and the amplification factor of RIS element satisfies $\eta_n > 1$. $\mathcal{P}_0$ and $\mathcal{P}_1$ are all non-convex optimization problems, which are difficult to be directly solved. Next, we propose effective algorithms to deal with them.

III. Joint Optimization Scheme for the Passive RIS

In this section, we first propose an AO algorithm based on SDR to solve $\mathcal{P}_0$, and then develop a low-complexity PDS technique to solve passive RIS BF.

A. Fix $\boldsymbol{\Theta}$ and Solve $\mathbf{w}$

Let's define

$$\begin{aligned}\mathbf{H}_U &= \left(\mathbf{h}_{AU}^H+\mathbf{f}_{AU}^H\boldsymbol{\Theta}\mathbf{G}_{AR}\right)^H\left(\mathbf{h}_{AU}^H+\mathbf{f}_{AU}^H\boldsymbol{\Theta}\mathbf{G}_{AR}\right)/\sigma_U^2,\\ \mathbf{H}_E &= \left(\mathbf{h}_{AE}^H+\mathbf{f}_{AE}^H\boldsymbol{\Theta}\mathbf{G}_{AR}\right)^H\left(\mathbf{h}_{AE}^H+\mathbf{f}_{AE}^H\boldsymbol{\Theta}\mathbf{G}_{AR}\right)/\sigma_E^2.\end{aligned} \tag{5}$$

Fixed $\boldsymbol{\Theta}$, and thus $\mathcal{P}_0$ can be recast to

$$\mathcal{P}_2 : \max_{\mathbf{w}} \ \frac{\mathbf{w}^H\mathbf{H}_U\mathbf{w} + 1}{\mathbf{w}^H\mathbf{H}_E\mathbf{w} + 1}, \text{ s.t. } \mathbf{w}^H\mathbf{w} \leq P_{\max}. \tag{6a}$$

According to [13], the optimal solution $\mathbf{w}^{\mathrm{o}}$ can be obtained as

$$\mathbf{w}^{\mathrm{o}} = \sqrt{P_{\max}}\mathbf{v}_{\max}\left[\left(\mathbf{H}_E+\frac{\mathbf{I}_{M_t}}{P_{\max}}\right)^{-1}\left(\mathbf{H}_U+\frac{\mathbf{I}_{M_t}}{P_{\max}}\right)\right], \tag{7}$$

where $\mathbf{v}_{\max}[\cdot]$ denotes the normalized eigenvector corresponding to the largest eigenvalue of its matrix.

B. Fix $\mathbf{w}$ and Solve $\boldsymbol{\Theta}$

Upon obtaining $\mathbf{w}$, $\mathcal{P}_0$ can be formulated as

$$\begin{aligned}\mathcal{P}_3 : \max_{\mathbf{u}} \ &\ln\left(1 + \mathbf{u}^H\mathbf{X}_U\mathbf{u}\right) - \ln\left(1 + \mathbf{u}^H\mathbf{X}_E\mathbf{u}\right) \quad (8a)\\ \text{s.t. } &|u_n| = 1, \forall n, u_{N_t+1} = 1, \quad (8b)\end{aligned}$$

where for $j \in \{U, E\}$, $\mathbf{F}_j = \mathrm{diag}\left(\mathbf{f}_{Aj}^H\right)\mathbf{G}_{AR}$, $\mathbf{X}_j = \frac{1}{\sigma_j^2}\begin{bmatrix}\mathbf{F}_j\mathbf{W}\mathbf{F}_j^H & \mathbf{F}_j\mathbf{W}\mathbf{h}_{Aj}\\ \mathbf{h}_{Aj}^H\mathbf{W}\mathbf{F}_j^H & \mathbf{h}_{Aj}^H\mathbf{W}\mathbf{h}_{Aj}\end{bmatrix}$, $\mathbf{u} = \left[\boldsymbol{\theta}^T, 1\right]^T = [u_1, \ldots, u_{N_t+1}]^T$, $\mathbf{W} = \mathbf{w}\mathbf{w}^H$. For convenience, we ignore $[\cdot]^+$ and adopt $\ln(\cdot)$ form.[2]

Obviously, we can denote variable $\mathbf{U} = \mathbf{u}\mathbf{u}^H$ and solve $\mathcal{P}_3$ with the SDR method [14]. However, this method needs to call the semidefinite program (SDP). Furthermore, it is found

[1] In fact, the transmit power of AP and RIS can be controlled by a common controller. Under the sum transmit power constraint, the transmit power of AP and RIS can be flexibly allocated according to the practical scenario.

[2] $[\cdot]^+$ denotes $\max\{\cdot, 0\}$, and thus $[\cdot]^+$ can be ignored because the SR should be non-negative.

that the optimal $\mathbf{U}^{\mathrm{o}}$ usually does not satisfy the rank-one constraint, and Gaussian randomization technique is required to construct the rank-one solution, but the required computational complexity becomes unaffordable for a large-size RIS.

To reduce the computational complexity for solving $\mathcal{P}_3$, we propose an MM algorithm. Specifically, given $\{\alpha^t, \beta^t\}$, refer to the inequality:

$$\begin{aligned}\ln\left(1+|\alpha|^2/\beta\right) \geq \ln\left(1+\left|\alpha^t\right|^2/\beta^t\right) - \left|\alpha^t\right|^2/\beta^t \\ + \frac{2\Re\left\{\alpha^t\alpha\right\}}{\beta^t} - \frac{\left|\alpha^t\right|^2\left(\beta+|\alpha|^2\right)}{\beta^t\left(\beta^t+\left|\alpha^t\right|^2\right)},\end{aligned} \tag{9a}$$

$$\ln\left(1+\frac{\alpha}{\beta}\right) \leq \ln\left(1+\frac{\alpha^t}{\beta^t}\right) + \frac{\beta^t}{\alpha^t+\beta^t}\left(\frac{\alpha}{\beta}-\frac{\alpha^t}{\beta^t}\right). \tag{9b}$$

Then, the lower bound of the user's rate can be expressed as

$$\begin{aligned}\ln\left(1+\mathbf{u}^H\mathbf{X}_U\mathbf{u}\right) \geq \ln\left(1+\hat{\mathbf{u}}^H\mathbf{X}_U\hat{\mathbf{u}}\right) - \hat{\mathbf{u}}^H\mathbf{X}_U\hat{\mathbf{u}} \\ + 2\Re\left\{\hat{\mathbf{u}}^H\mathbf{X}_U\mathbf{u}\right\} - \frac{\hat{\mathbf{u}}^H\mathbf{X}_U\hat{\mathbf{u}}\left(1+\mathbf{u}^H\mathbf{X}_U\mathbf{u}\right)}{1+\hat{\mathbf{u}}^H\mathbf{X}_U\hat{\mathbf{u}}},\end{aligned} \tag{10}$$

where $\hat{\mathbf{u}}$ is the solution of the last iteration $\mathbf{u}$. Similarly, we give the lower bound of $-\ln\left(1+\mathbf{u}^H\mathbf{X}_E\mathbf{u}\right)$ as follows

$$-\ln\left(1+\mathbf{u}^H\mathbf{X}_E\mathbf{u}\right) \geq -\ln\left(1+\hat{\mathbf{u}}^H\mathbf{X}_E\hat{\mathbf{u}}\right) - \frac{\mathbf{u}^H\mathbf{X}_E\mathbf{u}-\hat{\mathbf{u}}^H\mathbf{X}_E\hat{\mathbf{u}}}{\hat{\mathbf{u}}^H\mathbf{X}_E\hat{\mathbf{u}}+1}. \tag{11}$$

Omitting the constant term, we transform $\mathcal{P}_3$ into

$$\mathcal{P}_4: \min_{\mathbf{u}} \ \mathbf{u}^H\mathbf{A}\mathbf{u} - 2\Re\left\{\mathbf{u}^H\mathbf{B}\right\} \tag{12a}$$

$$\text{s.t.} \ |u_n| = 1, \forall n, u_{N_t+1} = 1, \tag{12b}$$

where $\mathbf{A} = \frac{\left(\hat{\mathbf{u}}^H\mathbf{X}_U\hat{\mathbf{u}}\right)\mathbf{X}_U}{1+\hat{\mathbf{u}}^H\mathbf{X}_U\hat{\mathbf{u}}} + \frac{\mathbf{X}_E}{\hat{\mathbf{u}}^H\mathbf{X}_E\hat{\mathbf{u}}+1}$, $\mathbf{B} = \mathbf{X}_U\hat{\mathbf{u}}$. According to the second-order Taylor expansion, the upper bound of the objective function of $\mathcal{P}_4$ can be expressed as

$$\begin{aligned}\mathbf{u}^H\mathbf{A}\mathbf{u} - 2\Re\left\{\mathbf{u}^H\mathbf{B}\right\} &\leq \mathbf{u}^H\bar{\mathbf{A}}\mathbf{u} + 2\Re\left\{\mathbf{u}^H\left(\mathbf{A}-\bar{\mathbf{A}}\right)\hat{\mathbf{u}}\right\} \\ &\quad + \hat{\mathbf{u}}^H\left(\bar{\mathbf{A}}-\mathbf{A}\right)\hat{\mathbf{u}} - 2\Re\left\{\mathbf{u}^H\mathbf{B}\right\} \\ &= 2\left(N_t+1\right)\lambda_{\max}\left(\mathbf{A}\right) - 2\Re\left\{\mathbf{u}^H\boldsymbol{\delta}\right\} - \hat{\mathbf{u}}^H\mathbf{A}\hat{\mathbf{u}},\end{aligned} \tag{13}$$

where $\bar{\mathbf{A}} = \lambda_{\max}\left(\mathbf{A}\right)\mathbf{I}_{N_t+1}$, $\boldsymbol{\delta} = \left(\bar{\mathbf{A}}-\mathbf{A}\right)\hat{\mathbf{u}} + \mathbf{B}$. Thus, ignoring the constant term, $\mathcal{P}_4$ can be further transformed as

$$\mathcal{P}_5: \max_{\mathbf{u}} \ \Re\left\{\mathbf{u}^H\boldsymbol{\delta}\right\} \quad \text{s.t.} \ (12\text{b}). \tag{14}$$

Obviously, by defining $\boldsymbol{\delta} = [\delta_1, \ldots, \delta_1]^T$, the maximum value can be obtained when the phase of δ_n and u_n are equal for any n. Thus, the closed-form optimal solution of $\mathcal{P}_5$ is given by

$$\mathbf{u} = \left[e^{j\arg(\delta_1)}, \ldots, e^{j\arg\left(\delta_{N_t}\right)}, 1\right]^T. \tag{15}$$

Then, $\hat{\mathbf{u}} = \mathbf{u}$ is updated until the inner loop objective function converges. $\mathbf{w}$ and $\mathbf{u}$ are updated in the outer loop until $\mathcal{P}_0$ converges to a locally optimal solution.

IV. Joint Optimization Scheme for the Active RIS

In this section, we first propose an AO algorithm based on SDR to solve $\mathcal{P}_1$, and then develop a low-complexity PDS technique to solve active RIS BF.

A. Fix $\boldsymbol{\Theta}$ and Solve $\mathbf{w}$

We first fix $\boldsymbol{\Theta}$, and then $\mathcal{P}_1$ can be transformed as

$$\mathcal{P}_6: \max_{\mathbf{W}} \ln\left(1+\mathrm{Tr}\left(\tilde{\mathbf{H}}_U\mathbf{W}\right)\right) - \ln\left(1+\mathrm{Tr}\left(\tilde{\mathbf{H}}_E\mathbf{W}\right)\right)$$

$$\text{s.t.} \ \mathrm{Tr}\left(\mathbf{W} + \mathbf{G}_{AR}^H\boldsymbol{\Theta}^H\boldsymbol{\Theta}\mathbf{G}_{AR}\mathbf{W}\right) \leq P_{\mathrm{I}}, \tag{16a}$$

$$\mathrm{Rank}\left(\mathbf{W}\right) = 1, \mathbf{W} \succeq 0, \tag{16b}$$

where $\mathbf{W} = \mathbf{w}\mathbf{w}^H$, $\tilde{\mathbf{H}}_j = \mathbf{H}_j \Big/ \left(\sigma_R^2/\sigma_j^2\left\|\mathbf{f}_{Aj}^H\boldsymbol{\Theta}\right\|^2+1\right)$ for $j \in \{U, E\}$, and $P_{\mathrm{I}} = \hat{P}_{\max} - \sigma_R^2\|\boldsymbol{\Theta}\|^2$. It is obvious that $\mathcal{P}_6$ is a non-convex optimization problem due to the non-convex objective function and rank-one constraint. To solve it, we first give the lower bound of the objective function based on the first-order Taylor expansion as follows

$$\begin{aligned}&\ln(1+\mathrm{Tr}(\tilde{\mathbf{H}}_U\mathbf{W})) - \ln(1+\mathrm{Tr}(\tilde{\mathbf{H}}_E\mathbf{W})) \geqslant \\ &\ln(1+\mathrm{Tr}(\tilde{\mathbf{H}}_U\mathbf{W})) - \ln(1+\mathrm{Tr}(\tilde{\mathbf{H}}_E\hat{\mathbf{W}})) \\ &-\mathrm{Tr}(\tilde{\mathbf{H}}_E(\mathbf{W}-\hat{\mathbf{W}}))/(1+\mathrm{Tr}(\tilde{\mathbf{H}}_E\hat{\mathbf{W}})) = \Gamma(\mathbf{W}, \hat{\mathbf{W}}),\end{aligned} \tag{17}$$

where $\hat{\mathbf{W}}$ is a fixed feasible point. Next, by dropping the rank-one constraint, $\mathcal{P}_6$ can be transformed the SDR problem

$$\mathcal{P}_7: \max_{\mathbf{W}} \ \Gamma(\mathbf{W}, \hat{\mathbf{W}}) \ \text{ s.t. } \mathbf{W} \succeq 0, (16\text{a}). \tag{18}$$

Therefore, $\mathcal{P}_7$ can be solved by the standard convex optimization technique. Finally, when $\mathbf{W}$ does not satisfy the rank-one constraint, a feasible rank-one solution $\mathbf{W}^*$ can be constructed by the Gaussian randomization method.

B. Fix $\mathbf{w}$ and Solve $\boldsymbol{\Theta}$

After obtain $\mathbf{W}$, $\mathcal{P}_1$ can be transformed as

$$\mathcal{P}_8: \max_{\boldsymbol{\theta}} \ \widehat{Z} - \breve{Z} \tag{19a}$$

$$\text{s.t.} \ \left\|\boldsymbol{\theta}^H\mathrm{diag}\left(\mathbf{G}_{AR}\mathbf{w}\right)\right\|^2 + \sigma_R^2\|\boldsymbol{\theta}\|^2 \leqslant P_{\mathrm{II}}, (4\text{c}), \tag{19b}$$

where $\widehat{\mathrm{Z}}$ and $\breve{\mathrm{Z}}$ are (20), $\mathbf{u} = \left[\boldsymbol{\theta}^T, 1\right]^T$, $P_{\mathrm{II}} = \hat{P}_{\max} - \mathrm{Tr}\left(\mathbf{W}\right)$.

For convenience, let's define

$$\begin{aligned}&\hat{\mathbf{X}}_j = \frac{1}{\sigma_j^2}\begin{bmatrix} \mathbf{F}_j\mathbf{W}\mathbf{F}_j^H + \hat{\mathbf{F}}_{Rj} & \mathbf{F}_j\mathbf{W}\mathbf{h}_{Aj} \\ \mathbf{h}_{Aj}^H\mathbf{W}\mathbf{F}_j^H & \sigma_j^2 + \mathbf{h}_{Aj}^H\mathbf{W}\mathbf{h}_{Aj}\end{bmatrix}, \\ &\qquad j \in \{U, E\}, \\ &\mathbf{H}_P = \begin{bmatrix} \mathrm{diag}\left(\mathbf{G}_{AR}\mathbf{w}\right)\mathrm{diag}(\mathbf{G}_{AR}\mathbf{w})^H + \sigma_R^2\mathbf{I} & \mathbf{0} \\ \mathbf{0} & 0\end{bmatrix}, \\ &\hat{\mathbf{F}}_{Rj} = \sigma_R^2\mathrm{diag}\left(\mathbf{f}_{Rj}^H\right)\mathrm{diag}\big(\mathbf{f}_{Rj}^H\big)^H, j \in \{U, E\}, \\ &\mathbf{V}_j = \frac{1}{\sigma_j^2}\begin{bmatrix} \hat{\mathbf{F}}_{Rj} & \mathbf{0} \\ \mathbf{0} & \sigma_j^2\end{bmatrix}, j \in \{U, E\}.\end{aligned} \tag{21}$$

$$\begin{aligned}\widehat{\mathrm{Z}} &= \ln\left(\mathbf{u}^H\mathbf{X}_U\mathbf{u} + \left\|\boldsymbol{\theta}^H\mathrm{diag}\left(\mathbf{f}_{RU}^H\right)\right\|^2\sigma_R^2/\sigma_U^2 + 1\right) + \ln\left(\left\|\boldsymbol{\theta}^H\mathrm{diag}\left(\mathbf{f}_{RE}^H\right)\right\|^2\sigma_R^2/\sigma_E^2 + 1\right), \\ \breve{\mathrm{Z}} &= \ln\left(\mathbf{u}^H\mathbf{X}_E\mathbf{u} + \left\|\boldsymbol{\theta}^H\mathrm{diag}\left(\mathbf{f}_{RE}^H\right)\right\|^2\sigma_R^2/\sigma_E^2 + 1\right) + \ln\left(\left\|\boldsymbol{\theta}^H\mathrm{diag}\left(\mathbf{f}_{RU}^H\right)\right\|^2\sigma_R^2/\sigma_U^2 + 1\right).\end{aligned} \tag{20}$$

$$
\begin{aligned}
&\widehat{\mathrm{Z}} \geq \ln\left(1+|\hat{\alpha}|^2\right)-|\hat{\alpha}|^2+2\Re\left\{\hat{\alpha}\bar{\alpha}\right\}-\frac{|\hat{\alpha}|^2\left(1+|\bar{\alpha}|^2\right)}{1+|\hat{\alpha}|^2}+\ln\left(1+|\hat{\beta}|^2\right)-|\hat{\beta}|^2+2\Re\left\{\hat{\beta}\bar{\beta}\right\}-\frac{|\hat{\beta}|^2\left(1+|\bar{\beta}|^2\right)}{1+|\hat{\beta}|^2},\\
&-\breve{\mathrm{Z}} \geq -\ln\left(1+\hat{z}\right)-\frac{z-\hat{z}}{\hat{z}+1}-\ln\left(1+\hat{\chi}\right)-\frac{\chi-\hat{\chi}}{\hat{\chi}+1}, |\hat{\alpha}|^2=\hat{\mathbf{u}}^H\mathbf{D}_U\hat{\mathbf{u}}, |\bar{\alpha}|^2=\mathbf{u}^H\mathbf{D}_U\mathbf{u},\\
&\left|\hat{\beta}\right|^2=\hat{\mathbf{u}}^H\hat{\mathbf{D}}_E\hat{\mathbf{u}}, \left|\bar{\beta}\right|^2=\mathbf{u}^H\hat{\mathbf{D}}_E\mathbf{u}, \hat{z}=\hat{\mathbf{u}}^H\mathbf{D}_E\hat{\mathbf{u}}, z=\mathbf{u}^H\mathbf{D}_E\mathbf{u}, \hat{\chi}=\hat{\mathbf{u}}^H\hat{\mathbf{D}}_U\hat{\mathbf{u}}, \chi=\mathbf{u}^H\hat{\mathbf{D}}_U\mathbf{u},\\
&\mathbf{D}_j=\frac{1}{\sigma_j^2}\begin{bmatrix}\mathbf{F}_j\mathbf{W}\mathbf{F}_j^H+\hat{\mathbf{F}}_{Rj} & \mathbf{F}_j\mathbf{W}\mathbf{h}_{Aj}\\ \mathbf{h}_{Aj}^H\mathbf{W}\mathbf{F}_j^H & \mathbf{h}_{Aj}^H\mathbf{W}\mathbf{h}_{Aj}\end{bmatrix}, \hat{\mathbf{D}}_j=\frac{1}{\sigma_j^2}\begin{bmatrix}\hat{\mathbf{F}}_{Rj} & \mathbf{0}\\ \mathbf{0} & 0\end{bmatrix}, j\in\{U,E\}.
\end{aligned}
\tag{25}
$$

Next, $\mathcal{P}_8$ can be reformulated as

$$\hat{\mathcal{P}}_8: \max_{\mathbf{U}} \ Z_S - Z_X \tag{22a}$$

$$\text{s.t. } \mathrm{Tr}\left(\mathbf{H}_P\mathbf{U}\right) \leqslant P_{\mathrm{II}}, \left|\mathbf{U}_{[n,n]}\right| \leqslant \beta_n^2, \forall n, \tag{22b}$$

$$\mathbf{U}_{[N_t+1,N_t+1]}=1, \ \mathrm{Rank}\left(\mathbf{U}\right)=1, \mathbf{U}\succeq 0, \tag{22c}$$

where $Z_S = \ln(\mathrm{Tr}(\hat{\mathbf{X}}_U\mathbf{U})) + \ln(\mathrm{Tr}(\mathbf{V}_E\mathbf{U}))$, $Z_X = \ln(\mathrm{Tr}(\hat{\mathbf{X}}_E\mathbf{U})) + \ln(\mathrm{Tr}(\mathbf{V}_U\mathbf{U}))$. Next, the lower bound of the objective function can be approximated as

$$
\begin{aligned}
&Z_S - Z_X \geq Z_S - \ln(\mathrm{Tr}(\hat{\mathbf{X}}_E\hat{\mathbf{U}})) - \ln(\mathrm{Tr}(\mathbf{V}_U\hat{\mathbf{U}}))\\
&-\frac{\mathrm{Tr}(\hat{\mathbf{X}}_E(\mathbf{U}-\hat{\mathbf{U}}))}{\mathrm{Tr}(\hat{\mathbf{X}}_E\hat{\mathbf{U}})} - \frac{\mathrm{Tr}(\mathbf{V}_U(\mathbf{U}-\hat{\mathbf{U}}))}{\mathrm{Tr}(\mathbf{V}_U\hat{\mathbf{U}})} = Z(\mathbf{U},\hat{\mathbf{U}}),
\end{aligned}
\tag{23}
$$

where $\hat{\mathbf{U}}$ is a fixed feasible point. Finally, we omit the rank-one constraint and $\hat{\mathcal{P}}_8$ can be rewritten as

$$\mathcal{P}_9: \max_{\mathbf{U}} Z\left(\mathbf{U},\hat{\mathbf{U}}\right) \text{ s.t. } (22\text{b}), (22\text{c}), (22\text{d}). \tag{24}$$

It is obvious that $\mathcal{P}_9$ is a convex SDR problem, which can be solved via the standard convex optimization technique. Similarly, we can obtain a rank-one solution by the Gaussian randomization method when it does not satisfy the rank one.

Here, $\mathbf{w}$ and $\mathbf{u}$ are updated until $\mathcal{P}_1$ converges to a locally optimal solution. However, this method still needs to call the SDR and construct the desired rank-one solution, which requires huge computational complexity for a large-size RIS. To reduce the computational complexity for solving $\mathcal{P}_8$, we propose a low-complexity PDS algorithm. Specifically, according to (9) we obtain the lower bound of $\widehat{Z}$ and $\breve{Z}$ as (25). Omitting the constant term, we transform $\mathcal{P}_8$ as

$$\mathcal{P}_{10}: \min_{\mathbf{u}} \mathbf{u}^H\hat{\mathbf{A}}\mathbf{u} - 2\Re\left\{\mathbf{u}^H\hat{\mathbf{B}}\right\} \tag{26a}$$

$$\text{s.t. } \mathbf{u}^H\mathbf{H}_P\mathbf{u} \leq P_{\mathrm{II}}, \tag{26b}$$

$$|u_n| \leq \beta_n, n\in\mathcal{N}, u_{N+1}=1, \tag{26c}$$

where

$$\hat{\mathbf{A}} = \frac{|\hat{\alpha}|^2\mathbf{D}_U}{1+|\hat{\alpha}|^2} + \frac{|\hat{\beta}|^2\hat{\mathbf{D}}_E}{1+|\hat{\beta}|^2} + \frac{\mathbf{D}_E}{\hat{z}+1} + \frac{\hat{\mathbf{D}}_U}{\hat{\chi}+1}, \tag{27a}$$

$$\hat{\mathbf{B}} = \mathbf{D}_U\hat{\mathbf{u}} + \hat{\mathbf{D}}_E\hat{\mathbf{u}}. \tag{27b}$$

Next, by introducing Lagrange multipliers $\zeta \in \mathbb{R}$, $\boldsymbol{\psi} \in \mathbb{R}^{(N_t+1)\times 1}$, $\rho_1 > 0$ and $\rho_2 > 0$, the augmented Lagrangian of (26a) can be expressed as

$$
\begin{aligned}
&\Gamma\left(\mathbf{u},\zeta,\boldsymbol{\psi}\right) = \mathbf{u}^H\mathbf{A}\mathbf{u} - 2\Re\left\{\mathbf{u}^H\mathbf{B}\right\} + \zeta\left(\mathbf{u}^H\mathbf{H}_P\mathbf{u} - P_{\mathrm{II}}\right)\\
&+\boldsymbol{\psi}^T\mathbf{G}\left(\mathbf{u}\right) + \frac{\rho_1}{2}\left\|\mathbf{u}^H\mathbf{H}_P\mathbf{u} - P_{\mathrm{II}}\right\|^2 + \frac{\rho_2}{2}\left\|\mathbf{G}\left(\mathbf{u}\right)\right\|^2,
\end{aligned}
\tag{28}
$$

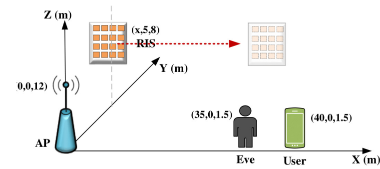

Fig. 2. Simulation deployment.

where $\mathbf{G}\left(\mathbf{u}\right)$ is defined as $\mathbf{G}\left(\mathbf{u}\right) = \left[G_1^+\left(\mathbf{u}\right), ..., G_{N_t+1}^+\left(\mathbf{u}\right)\right]^T$ with $G_n\left(\mathbf{u}\right) = \mathbf{u}^H\mathbf{E}_n\mathbf{u} - \beta_n$, $n\in\mathcal{N}$, $G_{N_t+1}\left(\mathbf{u}\right) = 0$, and $\mathbf{E}_n \triangleq \mathbf{e}_n\mathbf{e}_n^H$. Then, the iterative formula for $\hat{\mathbf{u}}$, $\hat{\boldsymbol{\psi}}$ and $\hat{\zeta}$ can be expressed as

$$\begin{bmatrix}\mathbf{u}\\ \boldsymbol{\psi}\\ \zeta\end{bmatrix} = \begin{bmatrix}\hat{\mathbf{u}}\\ \hat{\boldsymbol{\psi}}\\ \hat{\zeta}\end{bmatrix} - \hat{\nu}\begin{bmatrix}\nabla_{\mathbf{u}}\Gamma|_{\mathbf{u}=\hat{\mathbf{u}}}\\ -\nabla_{\boldsymbol{\psi}}\Gamma|_{\boldsymbol{\psi}=\hat{\boldsymbol{\psi}}}\\ -\nabla_{\zeta}\Gamma|_{\zeta=\hat{\zeta}}\end{bmatrix}, \tag{29}$$

where $\hat{\nu} > 0$ denotes the effective iteration step size, $\nabla_{\mathbf{u}}\Gamma$, $\nabla_{\boldsymbol{\psi}}$ and ∇_{ζ} are the iteration directions denoted by

$$
\begin{aligned}
&\nabla_{\mathbf{u}}\Gamma = \mathbf{A}\mathbf{u} - \mathbf{B} + \left(\zeta + \rho_1\left[\mathbf{u}^H\mathbf{H}_P\mathbf{u} - P_{\mathrm{II}}\right]^+\right)\Upsilon\left(\mathbf{u}\right)\\
&\quad + \sum\nolimits_{n=1}^{N_t+1}\left(\psi_n + \rho_2\left[G_n\left(\mathbf{u}\right)\right]^+\right)\mathrm{T}_n\left(\mathbf{u}\right),\\
&\nabla_{\boldsymbol{\psi}}\Gamma = \mathbf{G}\left(\mathbf{u}\right), \nabla_{\zeta}\Gamma = \mathbf{u}^H\mathbf{H}_P\mathbf{u} - P_{\mathrm{II}}.
\end{aligned}
\tag{30}
$$

Note that the auxiliary functions $\Upsilon\left(\mathbf{u}\right) \in \mathbb{C}^{(N_t+1)\times 1}$ and $\mathrm{T}_n\left(\mathbf{u}\right) \in \mathbb{C}^{(N_t+1)\times 1}$ are defined as

$$\Upsilon\left(\mathbf{u}\right) = \begin{cases}\mathbf{H}_P\mathbf{u}, \mathbf{u}^H\mathbf{H}_P\mathbf{u} - P_{\mathrm{II}} > 0\\ \mathbf{0}, \mathbf{u}^H\mathbf{H}_P\mathbf{u} - P_{\mathrm{II}} \leqslant 0\end{cases}, \tag{31a}$$

$$\mathrm{T}_n\left(\mathbf{u}\right) = \begin{cases}\mathbf{E}_n\mathbf{u}, \mathbf{u}^H\mathbf{E}_n\mathbf{u} - \beta_n > 0\\ \mathbf{0}, \mathbf{u}^H\mathbf{E}_n\mathbf{u} - \beta_n \leqslant 0\end{cases}, n\in\mathcal{N}, \tag{31b}$$

where $\mathrm{T}_{N_t+1}\left(\mathbf{u}\right) = \mathbf{0}$. By simultaneously updating $\mathbf{u}$, $\boldsymbol{\psi}$ and ζ until (28) converges, an optimal solution $\mathbf{u}^{\mathrm{opt}}$ can be obtained, which avoid the high complexity SDR approach.

Next, we analyze the computational complexity of the proposed methods. For the passive RIS, the computational complexity of the SDR method is $\mathcal{O}(I_o(M_t^3 + (N_t+1)^{3.5}))$, while that of the MM method is $\mathcal{O}(I_o(M_t^3 + I_i(N_t+1)^2))$, where I_o and I_i represent the number of iterations of outer loop and inner loop, respectively. For the active RIS, the computational complexity of the SDR method is $\mathcal{O}(I_o'(M_t^3 + (N_t+1)^{3.5}))$, while that of the PDS method is $\mathcal{O}(I_o'(M_t^3 + I_i'(N_t+1)^2))$, where I_o' and I_i' represent the number of iterations of outer loop and inner loop, respectively.

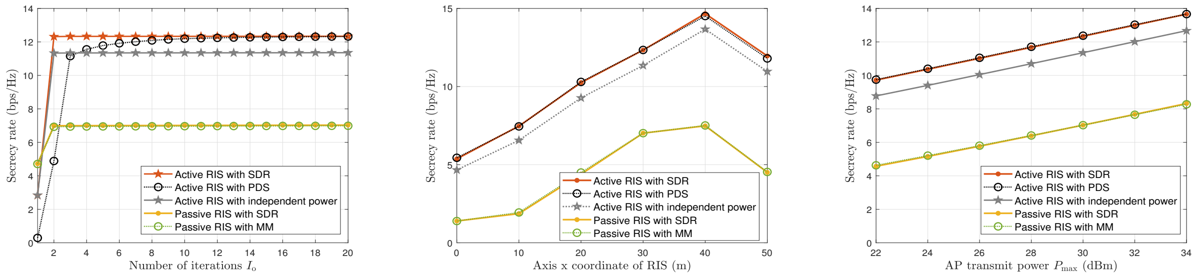

(a) (b) (c)

Fig. 3. (a) SR versus the number of iterations. (b) SR versus the x-axis coordinate of RIS. (c) SR versus transmit power $P_{\max}$.

V. Simulation Results

In this section, simulation are conducted to evaluate the performance of the proposed schemes. We assume that the user and Eve own the strong channel correlation for the AP, and then we change the RIS location to study the SR as shown in Fig. 2, namely the RIS location is moved from (0, 5, 8) m to (50, 5, 8) m. It is assumed that the three-dimensional coordinates of AP, user, Eve and RIS are (0, 0, 12) m, (40, 0, 1.5) m, (35, 0, 1.5) m and (x, 5, 8) m, respectively, where $x \in [0, 50]$. Let $L_{Aj} = 4$, $\alpha_{Aj}^{LoS} \sim \mathcal{CN}(0, \beta_{Aj}^2)$ and $\alpha_{Aj}^{NLoS} \sim \mathcal{CN}(0, 10^{-1}\beta_{Aj}^2)$ denote the path gain for LoS and non-line-of-sight (NLoS) [11], respectively, where $\beta_{Aj}\,[\mathrm{dB}] = PL\,(d_0) - 10\kappa_{Aj}\log_{10}(d^*/d_0)$. Here $PL\,(d_0) = -30$ dBm is the path loss of the reference distance $d_0 = 1$ m, and the channel link loss exponents are $\kappa_{Aj} = 3.5$, $\kappa_{Rj} = 2.8$ and $\kappa_{AR} = 2.2$, respectively [12]. We set $M_t = 8$, $N_t = 20$, $P_{\max} = \hat{P}_{\max} = 30$ dBm, $\sigma_U^2 = \sigma_E^2 = \sigma_R^2 = -80$ dBm, $\beta_n = 10$.

Fig. 3(a) shows the convergence behavior of different schemes, where we set $x = 30$. It is clear that all schemes converge quickly, and the SR of “Active RIS with SDR” and “Active RIS with PDS” schemes are almost the same and significantly superior to other schemes. Meanwhile, One can observe that the SR under the sum transmit power constraint is higher that under the independent power constraint. In addition, one can observe that the performance of the active RIS is better than that of the passive RIS as expected. The effect of the RIS deployment on the SR, as shown in Fig. 3(b) and Fig. 2. One can observe that when $x = 0$, namely RIS is close to AP, SR is the lowest for all schemes. It is because that the channels among AP/RIS to Eve/user still have strong correlation, and thus the SR is low. As x increases, the channel correlation of RIS to Eve and user decreases. In this case, the RIS can formulate more effective BF to user, improving the SR. We can observe that the SR is highest when $x = 40$ as shown in Fig. 3(b), it is also expected. Therefore, for the strong channel correlation case, different from the conventional scheme of the RIS deployment, RIS should be close to the user rather than the AP. Fig. 3(c) plots the SR versus maximum transmit power $P_{\max}$ for different schemes. Here, we set $x = 30$. As expected, SR increases with $P_{\max}$. Similarly, our proposed low-complexity MM and SDP schemes achieve almost the same performance as the corresponding SDR scheme.

VI. Conclusion

In this paper, we investigated how to optimally deploy RIS and joint design AP’s and RIS’s BF to improve the security under strong channel correlation. We proposed the effective beamforming optimization methods under passive and active RIS, respectively. The simulation results show that RIS can formulate more efficient BF for the user so as to improve the SR even when the channel between AP and Eve/ user have strong correlation. In addition, the active RIS is more conducive to the system security than the passive RIS.

References

[1] X. You, *et al.*, “Towards 6G wireless communication networks: Vision, enabling technologies, and new paradigm shifts,” *Sci. China-Inf. Sci.*, vol. 64, no. 1, pp. 5-78, Jan. 2021.

[2] W. Hao, *et al.*, “Securing reconfigurable intelligent surface-aided cell-free networks,” *IEEE Trans. Inf. Forensic Secur.*, vol. 17, pp. 3720-3733, Oct. 2022.

[3] X. Tang, *et al.*, “Securing wireless transmissions with RIS-receiver coordination: Passive beamforming and active jamming,” *IEEE Trans. Veh. Technol.*, vol. 70, no. 6, pp. 6260-6265, Jun. 2021.

[4] M. D. Renzo, *et al.*, “Smart radio environments empowered by reconfigurable intelligent surfaces: How it works, state of research, and road ahead,” *IEEE J. Sel. Areas Commun.*, vol. 38, no. 11, pp. 2450-2525, Nov. 2020.

[5] R. Long, *et al.*,“Active reconfigurable intelligent surface-aided wireless communications,” *IEEE Trans. Wireless Commun.*, vol. 20, no. 8, pp. 4962-4975, 2021.

[6] M. Di Renzo *et al.*, “Reconfigurable intelligent surfaces vs. relaying: differences, similarities, and performance comparison,” *IEEE Open J. Commun. Soc.*, vol. 1, pp. 798-807, 2020.

[7] Y. Ma, *et al.*, “Optimization for reflection and transmission dual-functional active RIS-assisted systems,” *arXiv preprint*, arXiv:2209.01986.

[8] G. Zhou, *et al.*, “Secure wireless communication in RIS-aided MISO system with hardware impairments,” *IEEE Wireless Commun. Lett.*, vol. 10, no. 6, pp. 1309-1313, Jun. 2021.

[9] M. Cui, *et al.*, “Secure wireless communication via intelligent reflecting surface,” *IEEE Wireless Commun. Lett.*, vol. 8, no. 5, pp. 1410-1414, Oct. 2019.

[10] H. Shen, *et al.*, “Secrecy rate maximization for intelligent reflecting surface assisted multi-antenna communications,” *IEEE Commun. Lett.*, vol. 23, no. 9, pp. 1488-1492, Sep. 2019.

[11] L. Dai, *et al.*, “Hybrid precoding-based millimeter-wave massive MIMO-NOMA with simultaneous wireless information and power transfer,” *IEEE J. Sel. Areas Commun.*, vol. 37, no. 1, pp. 131-141, Jan. 2019.

[12] L. Dong, *et al.*, “Active reconfigurable intelligent surface aided secure transmission,” *IEEE Trans. Veh. Technol.*, vol. 71, no. 2, pp. 2181-2186, Feb. 2022.

[13] A. Khisti and G. W. Wornell, “Secure transmission with multiple antennas I: The MISOME wiretap channel,” *IEEE Trans. Inf. Theory*, vol. 56, no. 7, pp. 3088-3104, Jul. 2010.

[14] Q. Wu and R. Zhang, “Intelligent reflecting surface enhanced wireless network via joint active and passive beamforming,” *IEEE Trans. Wireless Commun.*, vol. 18, no. 11, pp. 5394-5409, Nov. 2019.